# CHEMOSTRATIGRAPHY OF THE AUSTIN CHALK AND UPPER EAGLE FORD SHALE,SOUTH CENTRAL, TX

by

ZAIN ABDI

Presented to the Faculty of the Graduate School of

The University of Texas at Arlington in Partial Fulfillment

of the Requirements

for the Degree of

MASTER OF SCIENCE IN GEOLOGY

THE UNIVERSITY OF TEXAS AT ARLINGTON

May 2014

Acknowledgements

I would like to thank my Graduate Advising Professor, Dr. Harold Rowe, for giving me the opportunity to work under him. His patience, time, and energy were bountiful throughout this whole project, and it would have been unconceivable without his efforts. I would also like to thank Dr. Stephen Ruppel of the Texas Bureau of Economic Geology, Jacksons School of Geoscience (UT Austin), for providing the core and well log information for my research. I would like to thank James Donnelly, Nathan Ivicic, Kenneth Edwards, and Josh Lambert for their help in handling cores. My gratitude is also extended towards the professors on my committee, Dr. John Wickham and Dr. Andrew Hunt. Their insight and guidance on my Thesis project was invaluable. Furthermore, I would like to thank Sarah Allen for her help, assistance, and knowledge in the sequence stratigraphy interpretations of this project. A great deal of motivation and encouragement came from my close friend Rebecca Bryan who helped me keep my head up throughout this endeavor with her consistent adulation during our discussions regarding this project.

I would also like to thank UT Arlington's Geoscience Department for admitting me into their Graduate School Program.

February 6, 2014

Abstract

Chemostratigraphy Of The Austin Chalk And Upper Eagle Ford Shale

South Central Texas

Zain Abdi, M.S.

The University of Texas at Arlington, YYYY

Supervising Professor: Dr. Harold Rowe

A single drill core from La Salle, TX was analyzed for its chemical composition and percent concentration of both major and trace elements in order to understand depositional environments and local tectonic activity of the Balcones Fault Zone. The drill core contained the entirety of the Austin Chalk and the upper portion of the Upper Eagle Ford Shale. Samples were taken from 47 boxes at 3 inch intervals which accumulated in a total of 1,680 samples. Each sample was analyzed using a handheld x-ray fluorescence instrument which provided quantitative analysis of the following elements: Al, Ca, Cr, Cu, Fe, K, Mg, Mn, Mo, Ni, P, S, Si, Ti, and V. Furthermore, x-ray diffraction analysis was conducted at every 7 feet of the Austin Chalk and every 4 feet of the Upper Eagle Ford Shale. Calcium values ranged from 5% to 40% with the former values arising from the Upper Eagle Ford Shale and the latter values coming from the Austin Chalk. Sulfur percent composition ranged from 0%-20% and had similar trends as Magnesium which had values from 0.04% to 4.8%. The Austin Chalk contained great values of pyrite, illite, quartz, calcite, and dolomite. Trace element concentrations suggest that the depositional environment had periods of anoxic or euxinic events. Mineralogical and major elemental geochemistry suggests a carbonate rich Austin Chalk and calcareous Eagle Ford Shale.

Table of Contents

List of Illustrations

List of Tables

# Chapter 1

## Introduction

### 1.1 Energy-dispersive X-Ray Fluorescence

X-ray fluorescence has been used for many decades to produce a quantitative geochemical analysis (Norrish and Hutton, 1969; Potts and Webb, 1992; Tertian and Claisse, 1994; Fitton, 1997). However, there have been recent advancements in the technology behind X-ray fluorescence which has created a shift in the understanding of the chemistry of sedimentary rocks (Jansen et al., 1999; Haug et al., 2001; Rimmer, 2004; Richter et al., 2006; Tjallingii et al., 2007; Algeo and Maynard, 2008; Kujau et al., 2010; Tripathy et al., 2012). Modern advances in the thin window detector of current ED-XRF instruments along with miniaturization and stability of the x-ray tube, optimization and spot-size and collimator, engineering of stable digital pulse processing circuitry, and software development have created the ability for lower detection limits, instrument portability, and novel approaches to fundamental parameters (Rowe et al., 2012).

This study includes the energy-dispersive X-ray fluorescence (ED-XRF) of a single drill core from La Salle County, Texas. The drill core includes the entirety of the Austin Chalk and the upper portion of

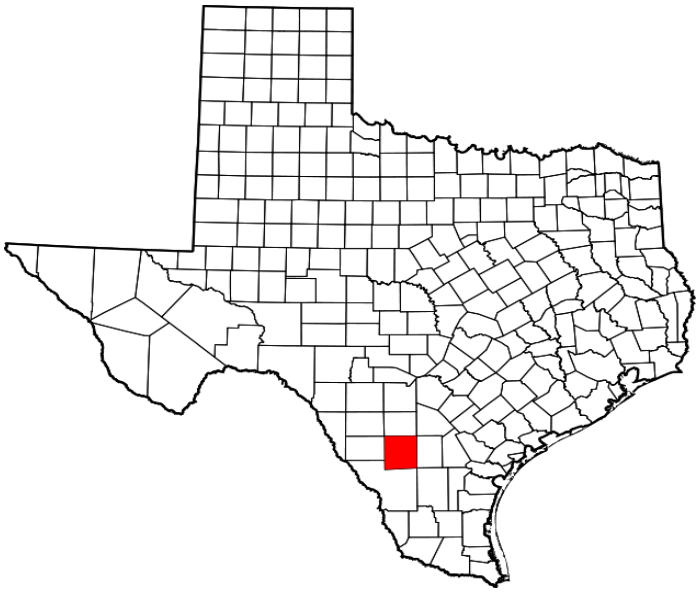

Figure 1-Location of La Salle County, Texas

the Eagle Ford Shale. Studying the geochemical data of the Austin Chalk and Eagle Ford Shale will provide a better insight as to what the depositional settings were for both formations. The study of sedimentary cyclicity has long attracted the interest of geoscientists because of its dual promise of enhancing chronostratigraphic resolution and of providing historical evidence for fundamental Earth processes such as climate and tectonics, interpreted through their roles as drivers of sedimentation (Locklair, 2007). A handheld XRF instrument was used on the Austin Chalk and Eagle Ford shale in order to gather a chemostratigraphic dataset. Geochemical proxy records for continental input (e.g., Si/Al, K/Al, Ti/Al) and bottom water oxygenation (Ni/Al, Zn/Al, V/Al) will show the correlation between geochemical data and sedimentary history (Flogel et al., 2008; Beckmann et al., 2005; Hofmann et al., 2003; Wagner et al., 2004).

The entire length of core measures approximately 600 feet, and the core was analyzed for this chemical composition at every three inch interval to produce a high resolution data set.

The combination of a high resolution chemostratigraphic dataset along with stratigraphy and biostratigraphy will provide a more in depth and conclusive understanding of the environmental conditions under which the Austin Chalk and Eagle Ford Shale were deposited.

## 1.2 Objectives

The data acquired for this project will be analyzed in order to provide an understanding of the Austin Chalk and Eagle Ford Shale's chemostratigraphy. Elemental chemistry signatures have been extensively used in literature as marine and environmental proxies to determine geochemical processes and conditions (Cruze and Lyons, 2004; Algeo and Maynard, 2008; Algeo and Rowe, 2012). The chemical concentrations obtained from the cores will help in the interpretation of the Austin Chalk and Upper Eagle Ford Shale's deposition may even provide the project with a story that will help explain paleoenvironmental conditions during the Late Cretaceous both on a global and local scale.

The main objects of the research are:

1) Develop a highly-resolved record of stratigraphic changes (chemostratigraphy) in the Austin Chalk and Upper Eagle Ford Shale.

2) Interpret the results in the context of changing depositional conditions along the lip of the Maverick Basin, South Texas, during the Late Cretaceous.

3) Place the interpretation in the context of documented regional and global changes that occurred during the Late Cretaceous.

## 1.3 Regional Setting

The most dominant structural feature of the western Gulf Coastal area is the Rio Grande embayment (Murray, 1961). Most of the embayment consists of Upper Cretaceous and Paleocene sediment (Murray, 1961; USGS, 1981). Toward the east, the Rio Grande Embayment merges with the San Marcos Arch; furthermore, the San Marcos Arch, an extension of the Llano Uplift is a broad, southeastward plunging structural high (USGS, 1981). The Austin Chalk and Eagle Ford Shale are deposits that extend across Texas from the northeast to the southwest, and these formations are carbon enriched mudstones and chalks that were deposited during the transgression of the Cretaceous sea in North America (Robison, 1997). Both the Austin Chalk and Eagle Ford Shale contain a noticeable amount of mica and clay. Dysaerobic to oxic depositional settings seem to be more characteristic of the Austin Chalk than the Eagle Ford shale because oxic environments do not favor the preservation of organic matter (Robison, 1997).

The Eagle Ford-Austin contact is conformable in southwestern and northern Texas, but the contact is disconformable in the central and north-central Texas areas (USGS, 1981). Both the Eagle Ford and Austin Chalk were deposited under the environmental conditions set by the Western Interior Seaway. Fluctuations in temperature, chemistry, and cyclicity of the Western Interior Seaway are seen in the deposition of these two formations.

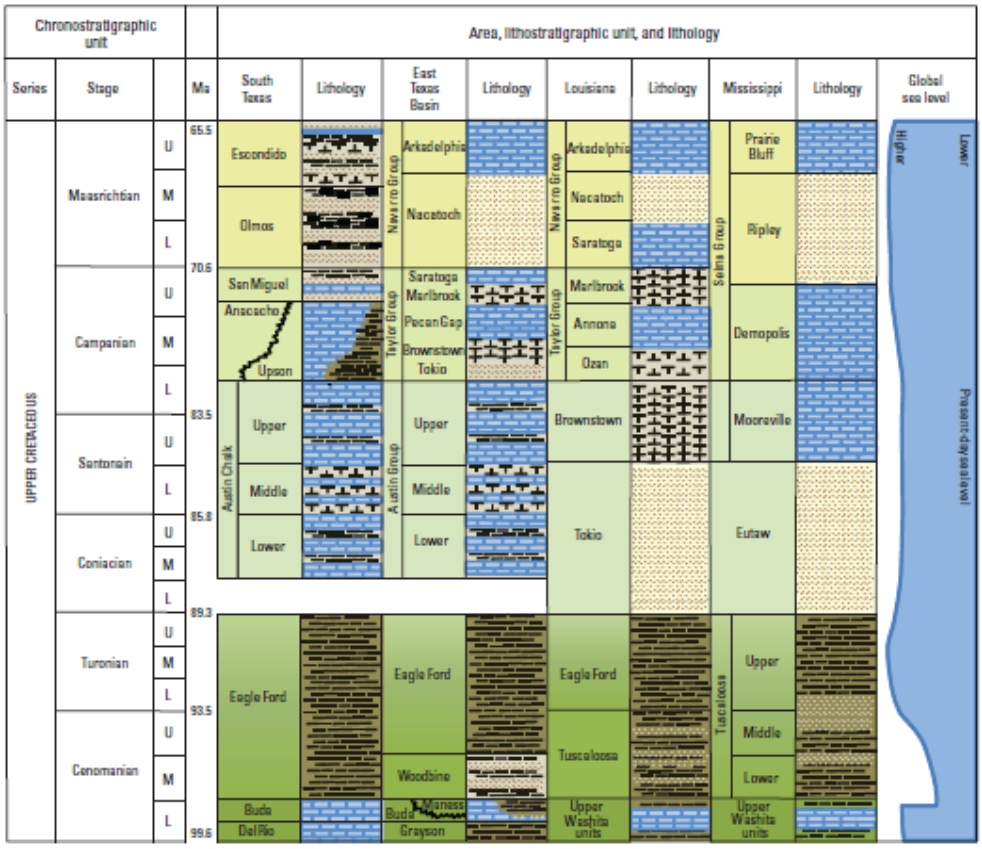


Figure 2 - Stratigraphic column for Upper Cretaceous rocks (modified from Vail et al., 1977; Wooten and Dunaway, 1977; Dawson and Reaser, 1990; Wescott and Hood, 1994; Mancini et al., 2006a,b). Global sea-level curve shows a prominent sea-level rise during the Cenomanian.

### 1.4 Cretaceous Western Interior Seaway

Learning the paleoenvironments of the Western Interior Seaway (WIS) is critically important in understanding the climatic development and subsequent sedimentological changes of North America throughout the Cretaceous (He et al., 2005). Therefore, the Western Interior Seaway has been the subject of geochemical investigation (Tourtelot, 1962; 1964; Tourtelot and Rye, 1969; Forester et al., 1977; Pratt, 1983; Wright, 1987; Whittaker et al., 1987; Whittaker and Kyser, 1993; Kyser et al., 1993; Pratt et al., 1993; Cadrin et al., 1996; He et al., 1996; Fisher and Arthur, 2002). Geochemical proxies

(Barrera and Savin, 1999; Barron, 1983; Douglas and Savin, 1975; Huber et al., 2002), the geographic extent of climatically sensitive terrestrial and marine flora and fauna (Habicht, 1979; Markwick, 1998), and studies of leaf physiognomy (Davies-Vollum, 1997; Heman and Spicer, 1997) suggest the Cretaceous greenhouse world was marked by high temperatures with a reduced equator-to-pole temperatures gradient (Barron, 1983; hay, 2008; Sloan and Barron, 1990) and elevated $CO_2$ concentrations (Arthur et al., 1985; Barron, 1985; Berner et al., 1993; Royer et al., 2001). This warmer climate would create large seas like the Western Interior Seaway (Barron, 1983; Hancock and Kauffman, 1979).

During the Cretaceous Period, the Western Interior of North America was an epicontinental sea that extended along a vast foreland basin, extending from the Gulf of Mexico to the Arctic Ocean and from Eastern British Columbia to western Ontario (Cumbaa et al., 2010; He et al., 2005). Both the Tethyan waters from the Gulf of Mexico and Boreal waters from the Arctic Ocean invaded the basin (He et al., 2005). The initial formation of the Western Interior Seaway started with the inundation of North America during the Aptian, but it did not become a continuous seaway until the late Aptian (Kauffman, 1984). The seaway was dynamic in terms of its width and depth, in response to changing sedimentological and tectonic processes (Kauffman, 1984). The Western Interior Seaway (WIS) extended 4,800 km North-South from the Arctic Ocean to the Gulf of Mexico and 1,600 km East-West with depths reaching over 300 m (Kauffman, 1984, 1977; Hancock and Kauffman, 1979; McDonough and Cross, 1991).

The highest sea levels of the WIS coincided with the peak in Cretaceous greenhouse temperatures between about 100 – 85 Ma (Huber et al., 1995, 2002), after which global cooling proceeded until the end of the Cretaceous (Barrera and Savin, 1999; Clarke and Jenkyns, 1999; Huber et al., 1995, 2002).

The structure of the WIS was a tectonically generated, deep foreland basin that was flanked by the Cordilleran thrust belt to the west, and an extensive, stable cratonic platform to the east (Price, 1973; Jordan, 1981; Kauffman, 1984; Miall et al., 2008). The tectonically active western margin was the source of most of the sediment coming into the sea, with coarse clastics depositing into rapidly prograding deltaic complexes within the subsiding basin (Cumbaa et al., 2010). The eastern margin was shallow in depth

and mostly sediment starved (McNeil and Caldwell, 1981; Schroder-Adams et al., 2001). The WIS received suspended fine clastics from the western basin, run-off from the low-lying hills of eastern North America, and the entirety of the WIS received volcanic ash from volcanoes on the tectonically active western margin (Kauffman, 1977).

Both the Austin Chalk and Eagle Ford Shale were deposited in the Western Interior Seaway. The geochemical data acquired from these two formations give an insight to the environmental conditions of the WIS, and how it was effected by terrigenous sediment run-off. The volcanic activity that occurred on the western portion of North America during the Cretaceous is evident in the formations in the form of ash beds.

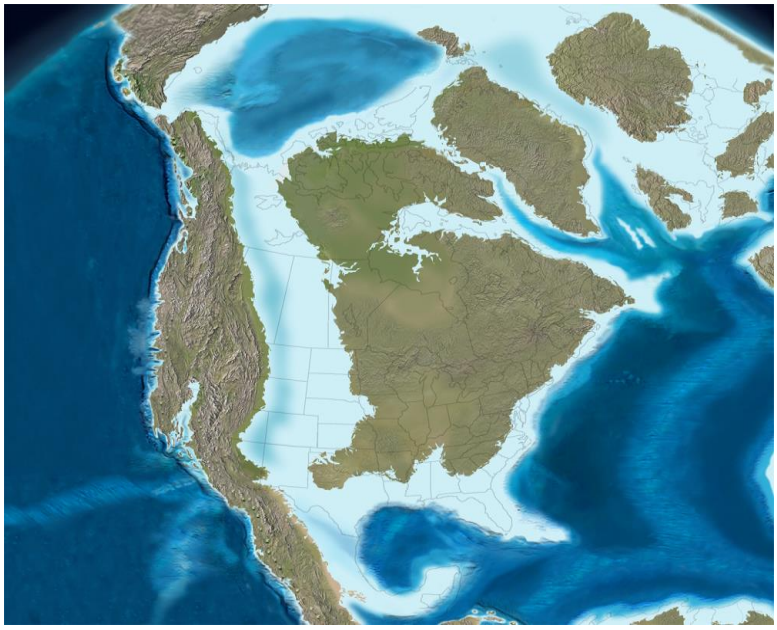

Figure 3 - A map of the Western Interior Seaway during the Late Cretaceous 85 Ma, after Blakey, 2013.

### 1.5 Ocean Anoxic Events (OAEs)

The Cretaceous period (145 – 66 Ma) is best known for major geological events such as Oceanic Anoxic Events (Schlanger and Jenkyns, 1976). There are three major OAEs that occurred during the Cretaceous: Aptian-Albian (OAE1), Cenomanian-Turonian (OAE2), and Coniacian-Santonian (OAE3) (Jenkyns, 1980; Bralower et al., 1994; Erba, 2004; Hu et al., 2012). The latter two OAEs occurred during the deposition of the Austin Chalk and Eagle Ford Shale. The former two events have been documented

to have oxygen depletion in oceanic bottom waters on a global scale (Schlanger and Jenkyns, 1976; de Gracianski et al., 1984; Schlanger et al., 1987; Sarmiento et al., 1988; Erba, 2004).

These events were triggered by changes in temperature, induced by rapid influx of $CO_2$ into the atmosphere from volcanogenic and/or methanogenic sources (Adams et al., 2010; Barclay et al., 2010). During the Cretaceous there were intense climatic conditions with extreme volcanic activity on land and underwater (Larson, 1991; Erba, 2004). The warmer climate of the Mid- to Late Cretaceous (Huber et al., 2002; Royer, 2006; Schouten et al., 2003) created greater thermal gradients leading to the creation of slower thermohaline circulations in the oceans (Schlanger and Jenkyns, 1976; Ryan and Cita, 1977; Fischer and Arthur, 1977).

The mechanisms that are used to explain the Oceanic Anoxic Events are: the decreased oxygen supply to the deep ocean due to slower oceanic circulation (Erbacher et al., 2001), and increased oxygen demand due to enhanced surface water productivity (Sarmiento et al., 1988; Handoh and Lenton, 2003). Volcanic activity is considered to be an indirect cause for the ocean anoxia by causing the warming of the atmosphere and ocean (Wagner et al., 2007). Increases in atmospheric temperatures directly relate to increases in precipitation which causes greater influxes of nutrients from land to ocean (Erbacher et al., 2001; Follmi, 1995, 1999; Handoh and Lenton, 2003; Wagner et al., 2007), and an increase in volcanic activity releases greater abundances of micronutrients to the deep sea (Erba, 2004).

Phosphorus is of particular interest in the initiation and termination of anoxic events. Furthermore, the indication of increased surface water productivity is evident by the increase in iron in black shales such as the Eagle Ford (Kuypers et al., 1999; Ohkouchi et al., 1999; Luning et al., 2003). The cycles of phosphorus and iron in the Western Interior Seaway will be depicted and discussed later.

## 1.6 Austin Chalk

The sequence of interbedded chalky limestone and marl overlying the Eagle Ford Group and underlying the Taylor Marl is herein referred to as the Austin Group (USGS, 1981).

### *1.6.1 Composition and Depositional Environment*

The Austin Group consists of interbedded thin to very thick bedded (0.3-1.5 m) chalk with thin intervening calcareous claystone (marl) layers (Dawson and Reaser, 1985). Various shallow and deep

marine fossils, benthic traces, and bioturbation have been preserved. Austin Chalk trace fossils occur as endogenic full-relief individuals filled with chalk, clay, or iron oxides (Dawson and Reaser, 1985). The Austin Chalk Formation in south-central Texas represents an “impure” depositional chalk within an environmental framework characterized by distinct paleobathymetric variations. Furthermore, the Austin Chalk is highly fossiliferous detrital chalk and is composed of a distinct planktonic microfossil assemblage (chiefly foraminifera and calcispheres) and finer nannofossils (coccoliths) which comprise much of the chalk’s micritic matrix (Dravis, 1981). Overall, the formation is chalk but is broken in several locations by ash layers.

Three main units of the Austin Chalk have been described in detail by Hovorka and Nance (1994). The lower chalk contains a number of lithofacies, including alternating chalk and marl with the chalk intervals having a greater thickness than the intervening marls. The middle marl contains a zone of alternating and cyclic burrowed chalk and light-colored marl, and authigenic clay that formed as an alternation product of volcanic ash is also present (Hovorka and Nance, 1994). The upper unit of the Austin Chalk is marked with an increase in winnowed packstone units and is considered to be a highstand deposit (Hovorka and Nance, 1994).

The carbonate deposition occurred in a shallow-marine setting, in paleowater depths that ranged from 30 ft to more than 300 ft, which indicates that deposition was below normal wave base on the inner to middle shelf as well as in much deeper waters (Dravis, 1979).

The Austin Chalk is Late Cretaceous in age and is found in South Texas and through parts of the Gulf Coast regions. The Austin Group (Coniacian-Santonian) is a sequence of interstratified chalk and marl deposited during the sea level highstand as a transgressive unit (Dawson et al., 1995; Hovorka and Nance, 1994).

The Austin uncomformably underlies the Taylor Marl (Campanian), and usually it has an uncomformable contact with the underlying Eagle Ford Shale (Montgomery, 1991). Generally the lower units of the Austin Chalk have greater shale content with increasing depth (Petroleum Frontiers, 1990b).

*1.6.2 Structure*

The Austin Chalk ranges in age from Coniacian to Santonian, and its formation thickness ranges from less than 100 feet to 600 ft in outcrop (Dravis, 1981; Hinds and Berg, 1990). Furthermore, the formation thickness below the surface ranges from 115 ft at its shallowest point to over 720 ft at its deepest (Petroleum Frontiers, 1990). In the Coniacian strata of the Austin Chalk there have been numerous disruptions of small scale faults (displacements of less than 3 meters) and closely spaced en-echelon joints with slickensides recording the movement along these faults (Dawson and Reaser, 1992).

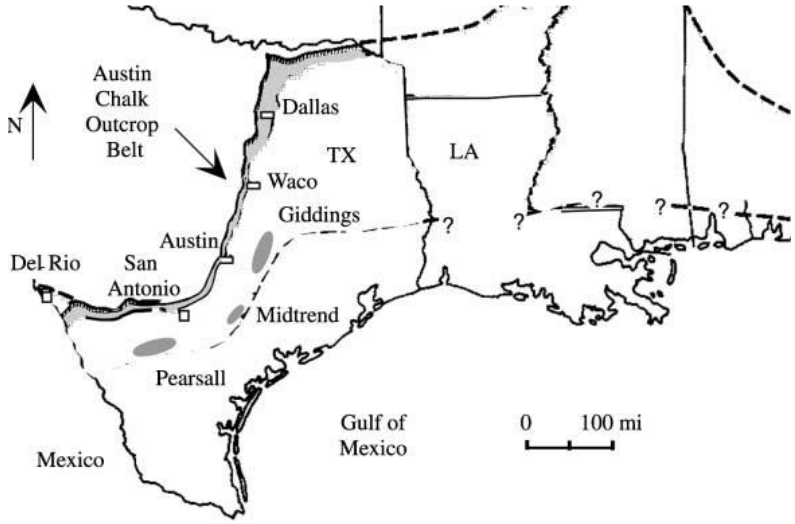


Figure 4 - Regional extent of Austin Chalk and equivalents, North American Gulf Cost. Light grey band indicates outcrop in Texas. The dashed line represents the extent of the Austin Chalk. The grey ovals represent the main oil fields within the Austin Chalk (Figure from Rijken and Cook, 2001.

## 1.7 Eagle Ford Shale

Calcareous sandstone, siltstone, calcareous shale, and flaggy limestone overlying the Woodbine Formation and conformable or disconformably overlain by the Austin Group are recognized herein as the Eagle Ford Group (USGS, 1981).

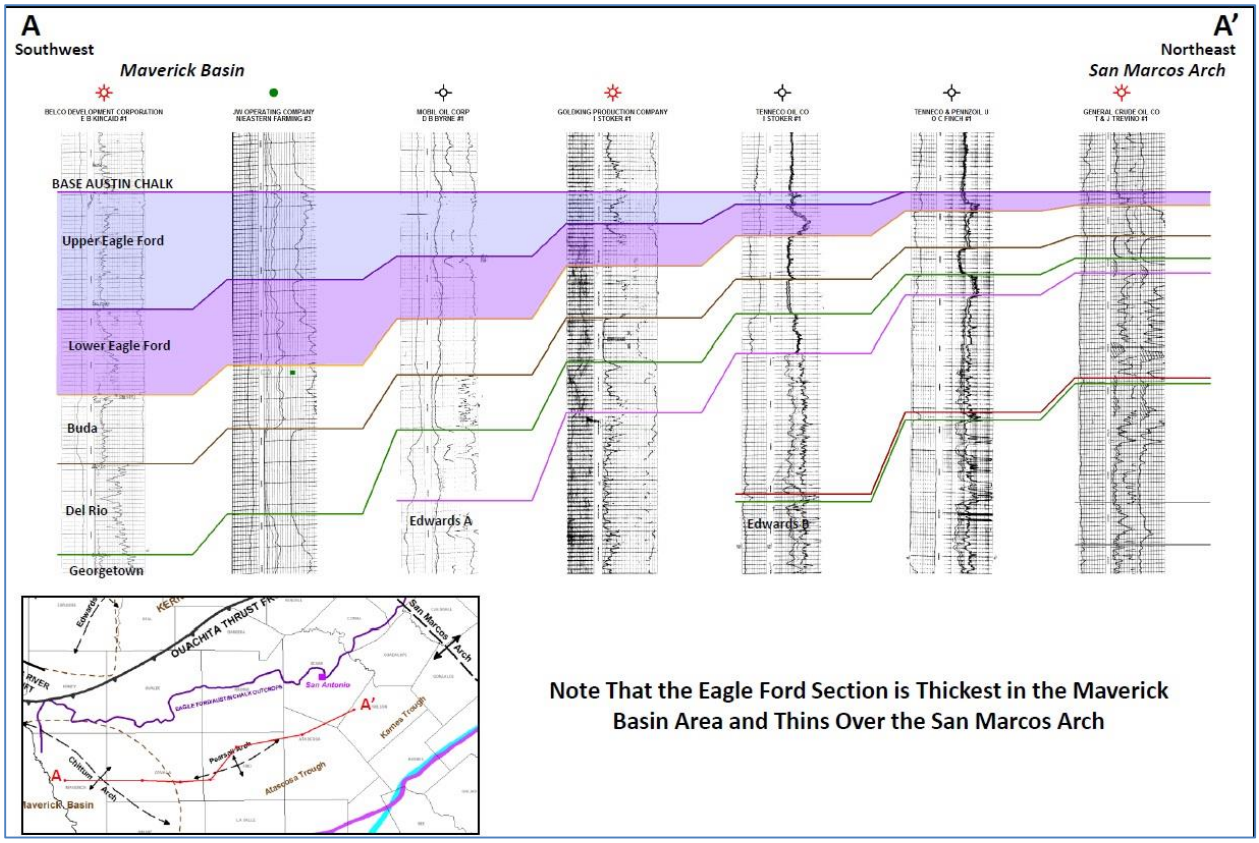


Figure 5 - Contact between Austin Chalk and Eagle Ford Shale.

*1.7.1 Composition and Depositional Environment*

Black shales (like the ones found in the Eagle Ford) are organic-rich, fine-grained deposits, which typically accumulate under anoxic-euxinic, deep water basinal locations (Demiason and Moore, 1980; Wignall and Maynard, 1993; Wingall and Newton 2000).

The Eagle Ford Shale reflects deposition of both siliciclastic and carbonate sediments during an early Late Cretaceous (Cenomanian-Turonian) transgression (Dawson et al., 1993).

The Upper Eagle Ford Shale is dark and fissile with a great abundance of aluminum and silica. Despite what is presented in its name, the Eagle Ford Shale is not true shale, and it contains a respectable amount of calcium. Eagle Ford outcrops near Austin, Waco and Dallas, Texas and subsurface equivalents in a core (Getty #1 J.T. Wilson) from LaSalle County, Texas reveals six microfacies: 1) pyritic shales; 2) phosphatic shales; 3) bentonitic shales; 4) fossiliferous shales; 5) silty

(quartzes) shales; and 6) bituminous claystone and shales (Dawson, 2000). Transgressive Eagle Ford shales consist mainly of microfacies 1, 4, and 6 while the Eagle Ford condensed interval consists of microfacies 1, 2, and 3, and lastly the highstand Eagle Ford shales are comprised of microfacies 4 and 5 (Dawson, 2000). This formation's interval is characterized by overall lower gamma-ray values and consists of interbedded dark and light gray calcareous mudrock, and the upper zone is in distinctly gradational contact with the Austin Chalk, consistent with observations from cores (Hentz and Ruppel, 2010).

The Austin/Eagle Ford contact represents the Turonian/Coniacian boundary (89 MA) with the Cenomonian/Turonian (92 MA) boundary occurring within the Eagle Ford Group (Dawson, 2000). The core samples observed in this project were taken deep beneath the surface in order to obtain genuine results and not results manipulated or destroyed by weathering or erosion processes. The unit, as thick as ~660 ft in the western Maverick Basin, gradually thins northeastward toward the San Marcos Arch and then thickens northeastward of the arch (Hentz and Ruppel, 2010).

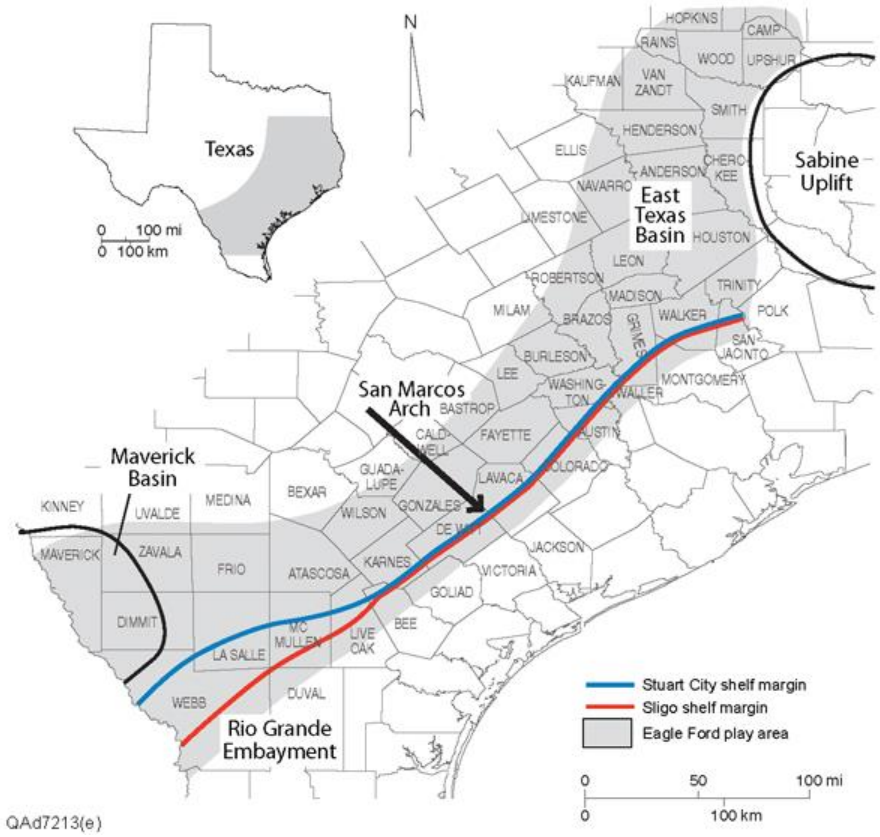


Figure 6 - Location of the Eagle Ford Shale.

*1.7.2 Structure and Location*

The Eagle Ford Shale extends north of Sherman County to down south of Del Rio, Texas. The thickness of the Eagle Ford is dependent on the regional geologic settings. In the vicinity of Austin, Travis County, the Eagle Ford thins considerably owing to the proximity of the San Marcos Arch (USGS, 1981).

In southern Texas near Del Rio, the Eagle Ford thickens in the Rio Grande Embayment (Maxwell et al. 1967).

The full Eagle Ford Shale has yet to be defined; depth, thickness, and rock characteristics of the unit across its subsurface area of occurrence provide a first approximation of potential producing areas (Hentz and Ruppel, 2010). Even though the project is limited to the upper portion of the Eagle Ford, it does provide a good insight of the transition from the Austin Chalk into the Eagle Ford. Within the Maverick Basin/Rio Grande Embayment area, the Eagle Ford Shale extends from outcrop to as deep as

~15,600 ft in northeast Webb County at the limit of deep well coverage at the Sligo shelf margin (Hentz and Ruppel, 2010).

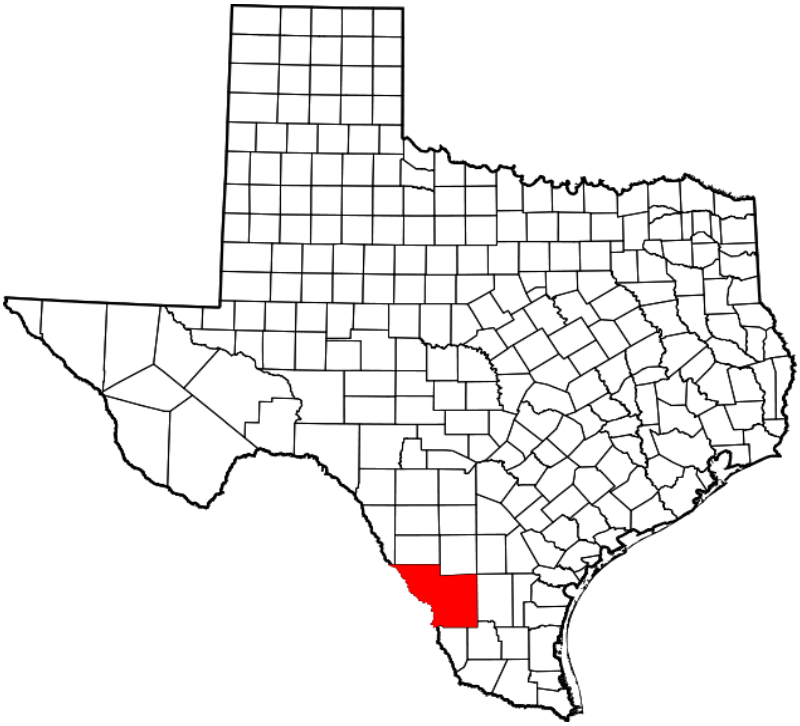

Figure 7 - Location of Webb County

# Chapter 2

# Methods

## 2.1 Drill Core Information

A single drill core from La Salle, Texas aged Late Cretaceous was studied. The core description is shown in the table below.

Table 1 - Summary of drill core.

| | Getty Hurt |
|---|---|
| **Location** | La Salle County, Texas |
| **Austin Chalk/Eagle Ford Interval (ft)** | 6,732 – 7,303 |
| **Box Numbers** | 1-47 |
| **Number of Samples** | 1,664 |
| **Core Condition** | Cut (half, quarter) |
| | |

The data acquired from the XRF instrument will include both major and trace elements. The major element data will provide information on major fluxes to and within the WIS waters. The trace elements give an insight on changes in ocean chemistry typically during anoxic events and major ocean circulations/overturns.

## 2.2 Energy dispersive X-Ray Fluorescence (ED-XRF)

A Bruker handheld energy dispersive X-ray fluorescence instrument was used to calculate percent elemental chemistry of the core at every three inch interval. The instrument was kept stationary, and parts of the drill core were placed on top of the instrument's 3 x 4 mm window in order to analyze the sample's percent composition. Each sample was cleaned using a carbon fiber fabric in order to remove any contamination. A flat sample surface is necessary because accuracy of the ED-XRF diminishes with greater distance from the silicon detector (SiPIN) which is located below the sampling window (Hughes, 2011).

Each sample was run twice in order to measure major and trace elements. The major elements were measure for 60 seconds for each sample, and trace elements were measured for 90 seconds for each sample. A vacuum pump was used to remove any air that was between the sampling window and the detector.

The entirety of the core was marked at every three inches, so the major and trace element sampling was taken at the exact same marking.

*2.2.1 Calibration of the ED-XRF*

At the beginning and end of each sampling session, a calibration method was used. A pressed pellet with known elemental percent composition was run three times for 180 seconds each.

All of the 270 major element X-ray spectra were loaded into the Bruker CalProcess software along with a reference table with known accepted elemental concentration values for each element, and for each element a slope and background inter-element correction was performed (Pukar, 2011). Any of the values that did not fall in the 95% confidence level were removed. Another calibration process followed after the first calibration curves were created, and a statistical analysis of each element calibration curve was performed.

The major element calibration included: Calcium, Aluminium, Magnesium, Silicon, Sulfur, Phosphorus, Potassium, Titanium, Vanadium, and Chromium.

The trace element calibration included: Cobalt, Nickel, Copper, Zinc, Thorium, Rubidium, Uranium, Strontium, and Molybdenum.

# Chapter 3

## Results

*Figure 8:*

This figure shows the percent elemental composition of major elements: Ca and Al. The Si/Al indicates the quartz clay ratio. This ratio shows the upper Austin Chalk being high in quartz level relative to the rest of the formation.

The boundary between the Austin Chalk and Eagle Ford Shale is indicated at approximately 7220 feet. The boundary is associated with a ~10% drop in Ca and a ~2% increase in Al when moving from the Austin Chalk to the Eagle Ford Shale. Despite the fact that the Eagle Ford is a black shale, its composition suggests that the shale is mostly calcareous.

*Figure 9:*

%S and %Mg are marked at four locations within the core. These markings show the correlation in the increase in %S occurring in association with an increase in %Mg. Overall, these two elements share the same oscillations in the middle of the Austin Chalk. It should be noted that these oscillations do not occur in the upper or lower parts of the Austin Chalk, and they do no occur in the Eagle Ford Shale. Furthermore, %P also has the same oscillations as S and Mg which suggests a correlation between the three elements.

*Figure 10:*

The chemostratigraphy of Ti, K, and Fe. There is no correlation apparent in these three graphs as seen versus depth. However, correlations do come apparent when plotted against each other as shown in Figures 13a – 13c.

There is no significant oscillation of Fe in the Austin Chalk, but Fe does increase in concentration through the Eagle Ford. Pyrite was not observed in the core, and it should be noted that S and Fe do not share the same oscillations that S and Mg do.

*Figure 11:*

This figure is a ternary diagram of clay, silica, and carbonate using normalized calcium oxide (CaO), aluminum oxide ($Al_2O_3$), and silica dioxide ($SiO_2$). The Ca-Al-Si ternary is used to compare major shale components (Brumsack, 1989).

This type of ternary diagram is typically used to show the variation of quartz, clay, and calcite in mudrocks. However, the Austin Chalk data is also included in this ternary diagram, so it depicts a bias towards carbonates.

*Figure 12:*

This figure contains trace elements Zn, Cu, and Ni. The data is presented in PPM. Originally, the XRF measures element composition in percent. The percent can be converted to PPM by dividing the percent composition by a factor of 10,000. The trace metals are presented in PPM because it provides better clarification.

There are no distinct oscillations of these traces elements in the Austin Chalk. However, in the Eagle Ford the trace elements do increase in the upper portion.

Trace elements have often been used as proxies about paleoenvironmental conditions by many researchers (Dean and Arthur, 1989; Zheng et al., 2000; Rimmer, 2004; Tribovillard et al., 2006; Algeo et al., 2003, 2006; Brumsack, 2006; Algeo and Maynard, 2008; Rowe et al., 2008; Algeo and Tribovillard, 2009; Piper and Calvert, 2009).

*Figure 13:*

A: Ti/Al – A Ti and Al  positive trend is used as a proxy for detrital indicators.

B: Ti/Fe – Using the Ti and Fe association can be used as a proxy for clay provenance. The positive correlation here is explain with Figure 13 D.

C: Ti/K – Affiliation of Ti with clay is depicted by the relationship of Ti over K. Here Ti and K make a positive correlation, so Ti does increase with increase clay content.

D: Fe/Al – The positive association of Fe and Al along with the positive association of Ti and Fe indicates a clay provenance to be both detrital and terrestrial. Furthermore, the Fe/Al correlation can also be used as an anoxia indicator.

E: Si/Al – Silica and Al ratio scatter plot depicts a positive correlation which suggests that with an increase Al there is an increase in Si.

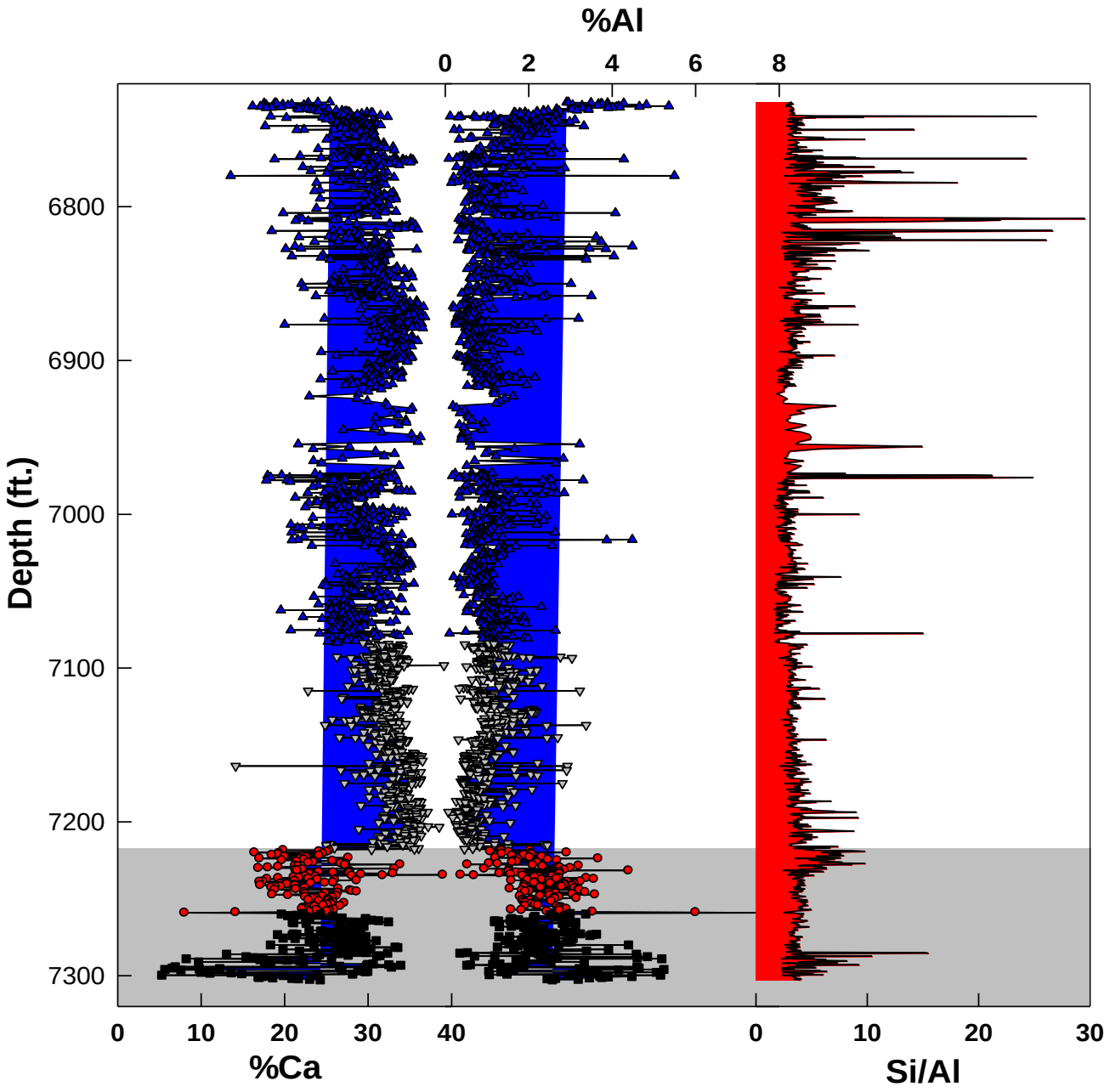


Figure 8 - Chemostratigraphy of Austin Chalk and Eagle Ford Shale's calcium and aluminum. The third column is the quartz/clay ratio. Gray band indicates the Eagle Ford Shale.

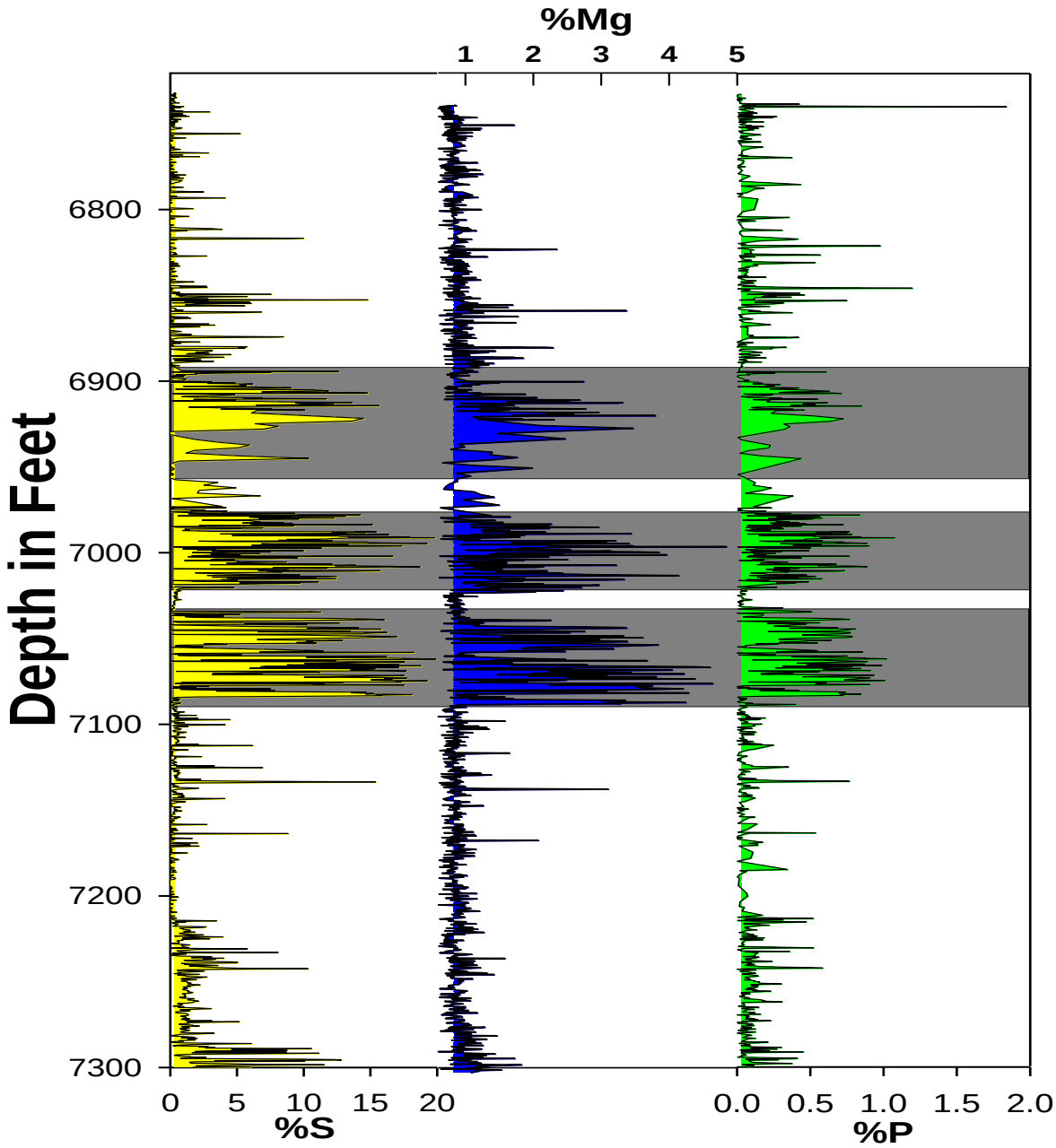


Figure 9 - Chemostratigraphy of sulfur, magnesium, and phosphorus. Dark gray bands indicate correlations in the three graphs.

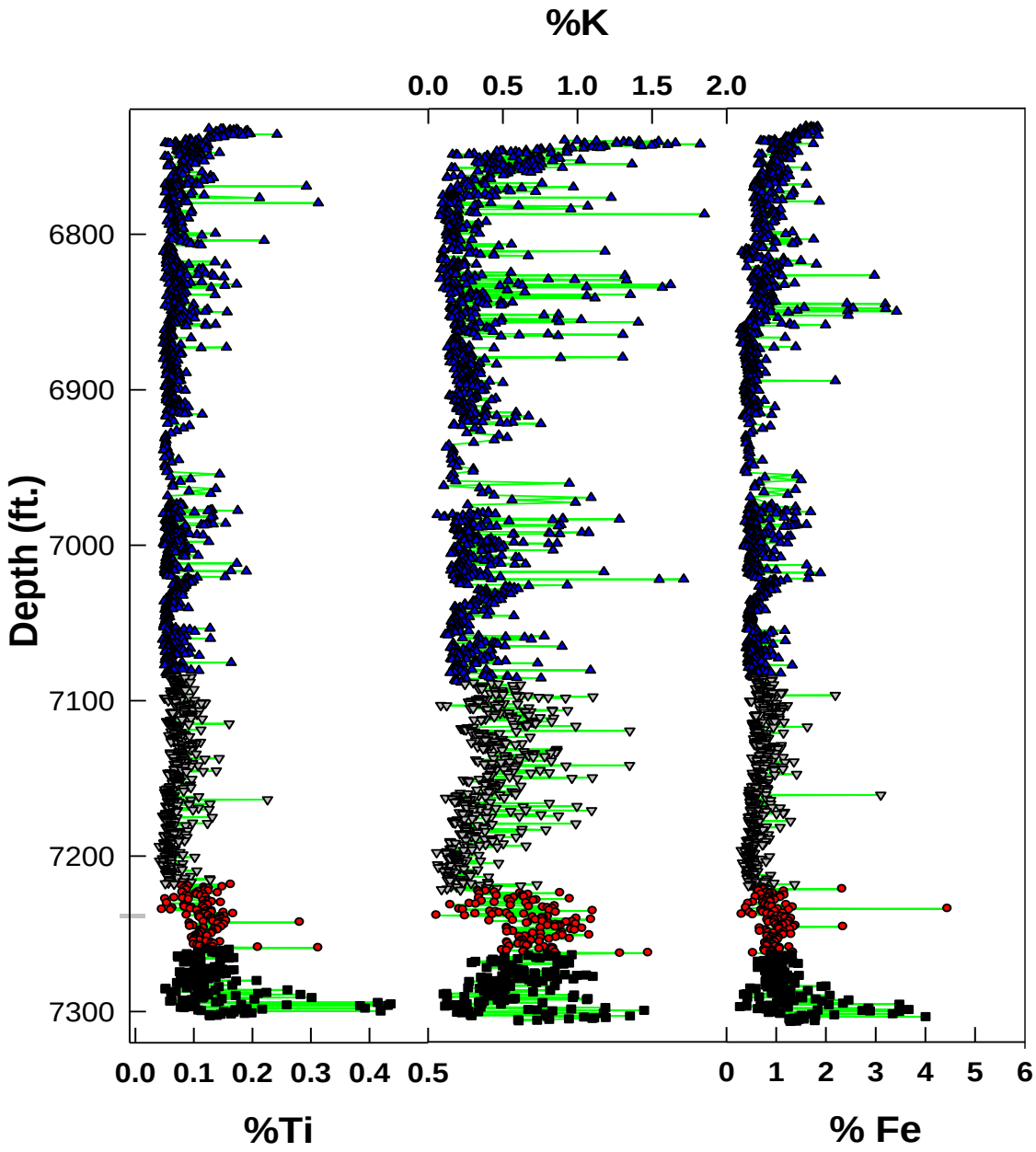


Figure 10 - Chemostratigraphy of the trace metals titanium, potassium, and iron. Gray band depicts the Eagle Ford Shale.

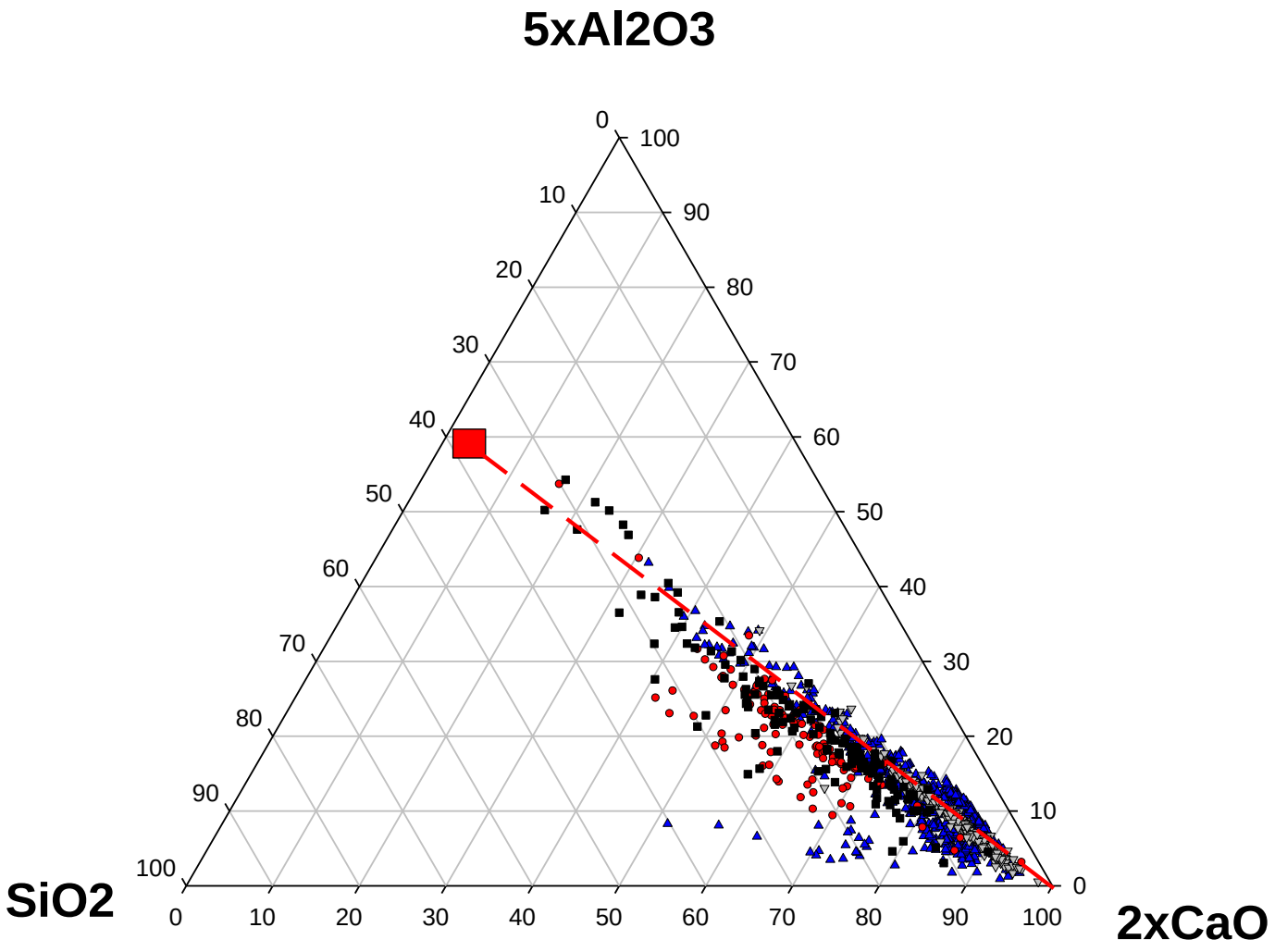


Figure 11 - Si-Al-Ca ternary diagram of the Austin Chalk and Eagle Ford Shale.

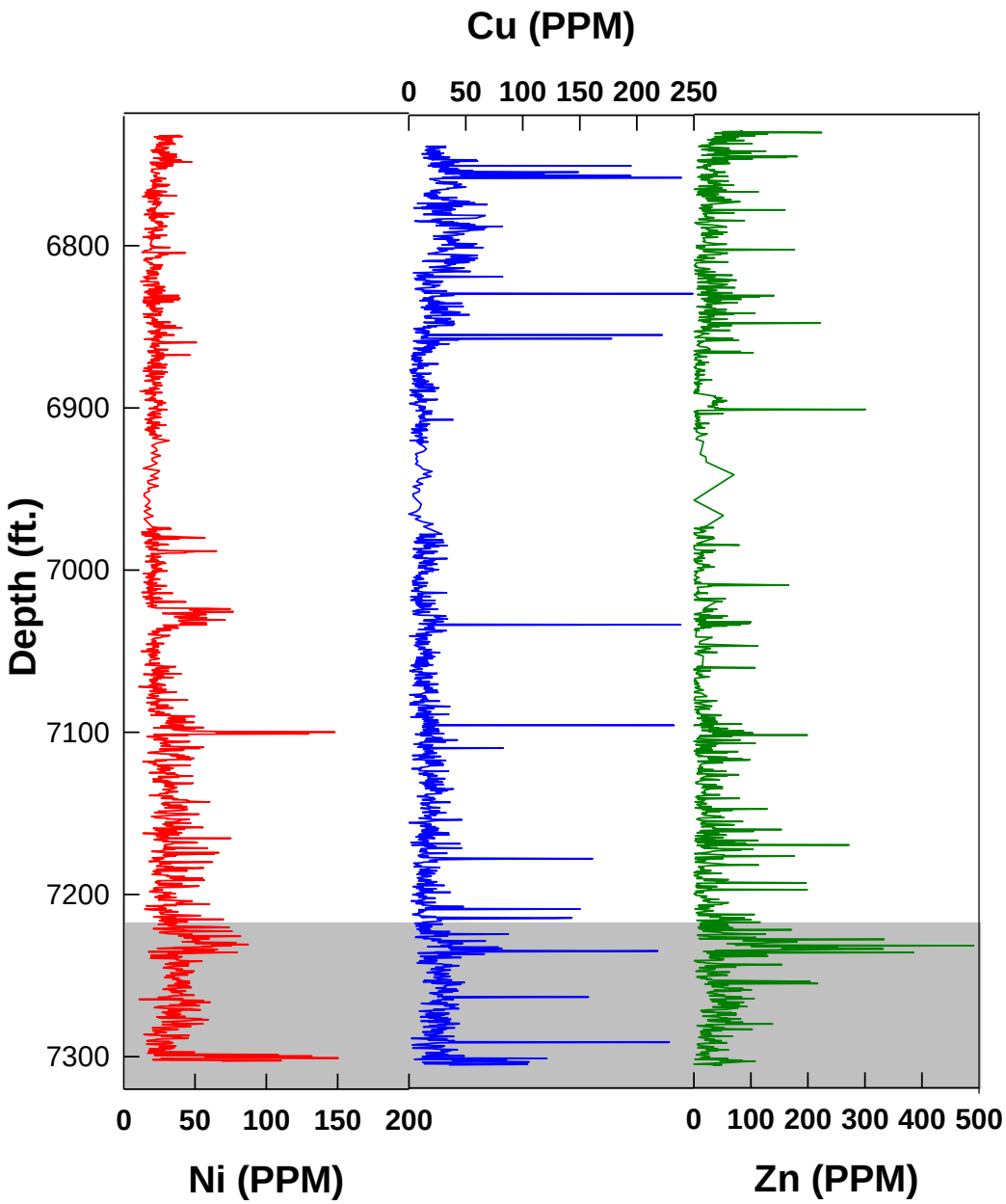


Figure 12 - Chemostratigraphy of trace elements: nickel, copper, and zinc presented in parts per million.

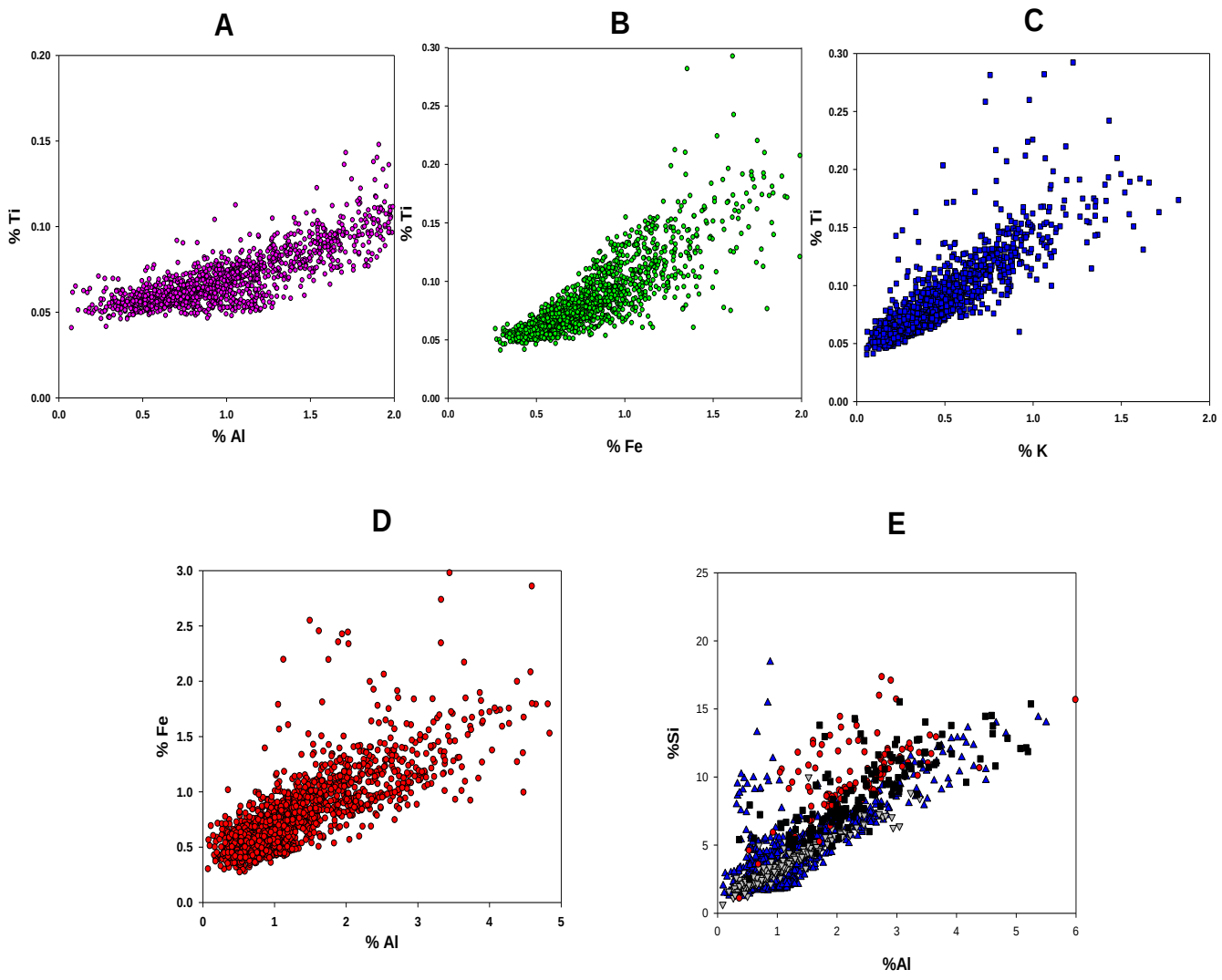


Figure 13 - Cross plots of A) Ti/Al, B) Ti/Fe, C) Ti/K, D) Fe/Al, E) and Si/Al.

# Chapter 4

# Discussion

The Austin Chalk and Eagle Ford Shale formations will be compared to several other formations in order to better understand the implications of geochemical variations found in the Austin Chalk and Eagle Ford. The X-ray fluorescence of detrital (Al, Ti, Zr), carbonate (Ca, Mg, Mn, Sr), and organic associations (Zn, Ni, Cu, Fe) will be evaluated individually and as a whole.

## 4.1 Major and Trace Elements

The major elements included in this study are: Aluminum (Al), Calcium (Ca), Iron (Fe), Potassium (K), Magnesium (Mg), Manganese (Mn), Phosphorus (P), Titanium (Ti), and Sulfur (S). The trace elements are: Copper (Cu), Nickel (Ni), and Zinc (Zn). Trace elements such as Uranium (U) and Molybdenum (Mo) were excluded from this study due to their extremely low to values that often ranged in negatives. Since it is impossible to have a negative value for an element in a rock, the overall data was excluded. Nevertheless, trace elements do have an important value in geochemical research. These elements are often linked to biological processes, and they have been used to reach various paleoenvironmental conclusions by various researchers (Dean and Arthur, 1989; Zheng et al., 2000; Rimmer, 2004; Tribovillard et al., 2006; Algeo et al., 2003, 2006; Brumsack, 2006; Algeo and Maynard, 2008; Rowe et al., 2008; Algeo and Tribovillard, 2009; Piper and Calvert, 2009).

## 4.2 Detrital Elements

Detrital information can mostly be extrapolated from the Si/Al ratio which is a quartz/clay indicator (Tribollivard et al., 1994; Caplan and Bustin, 1998; Murphy et al., 2000; Rimmer et al., 2004). Figure 8 contains a Si/Al relationship, there is a noticeable difference between the Upper Austin and the Upper Eagle Ford. The high data points that are seen in the Upper Austin indicates minerals that are silicate minerals that are not clay (quartz is an example). Whereas throughout the Mid- Lower Austin Chalk and Eagle Ford, there are abundant amounts of clay minerals. Figure 11 shows a strong Si/Al relationship in both the

Austin Chalk and Eagle Ford, and the data points that lay about the overall trend are associated with the high data points that are seen in the Si/Al ratio from Figure 8.

The difference in quartz/clay ratio between the Upper Austin Chalk and the rest of the available data suggests that during the brief time in Late Cretaceous the influx of detrital sediments from terrigenous sources came from more silica based provenance rocks. Another scenario that would explain the increase in quartz in the Upper Austin Chalk could be the increase in biogenic silica. Fossil remains found in the upper portion of the Austin Chalk core indicate that the quartz could have come from planktonic microfossil assemblage (chiefly foraminifera and calcispheres) and finer nannofossils (coccoliths) as mentioned above.

In order to discern between terrigenous or biogenic sources of the quartz in the Upper Austin Chalk, are correlation between Al and Ti is needed. This is because Al and Ti are immobile during diagenesis (Tribovillard et al., 2006). Furthermore, Al is typically not effected by any biological or diagenetic process, and it has very low concentrations in seawater (Brumsack, 2006; Orians and Bruland, 1986). Ti, on the other hand, is typically found in clay or sand size minerals such as ilmenite, rutile, and augite (Calvert 1976; Shimmield, 1992; Rimmer et al., 2004).

Based on the attributes of Al and Ti, the Ti/Al ratio can be used as a proxy for paleo-wind strength (Shimmield, 1992; Rimmer et al., 2004). Stronger winds can carry coarser grained particles, and a higher Ti amount could be attributed to stronger paleo-winds.

However, there is no indication of a strong correlation positive correlation between Al and Ti. Therefore, it can be inferred that the high data points of Si/Al in the Upper Austin Chalk originate from a biogentic source rather than a terrigenous.

Figure 14 depicts the relationship between Aluminum and Iron where Aluminum is a proxy for clay. Since there is a positive correlation between the Fe/Al ratio, it can be determined that Fe is associated with the clay particles. Clay minerals that contain iron are: illite or chamosite.

Calcium rich percentages are found abundantly in the Austin Chalk and decrease during the transition from the Austin Chalk to the Eagle Ford. Calcium levels are seen to be indirectly proportional to Aluminum levels. In the Austin Chalk the Calcium is seen in calcite and dolomite for the most part, and the shift from Ca-majority rocks to Al-majority rocks begins in the Lower Austin Chalk with a distinct transition at the Austin Chalk/Eagle Ford boundary.

When Sulfur-Magnesium-Phosphorus are plotted together, a distinct relationship becomes apparent. All three of these elements share the same trend and oscillations. There are four spikes in the S-Mg-P chemostratigraphic graphs which suggests that these three elements are being affected by the same environmental processes.

As mentioned before, Phosphorus appears to play a key role in the associations of the three elements. Accumulating evidence from various core records suggest that changes in Phosphorus cycles may have been of particular importance for the initiation and termination of periods of oceanic anoxic events (Tsandev and Slomp, 2009). There are two examples that explain why Phosphorus can trigger and end OAEs. 1) The increased availability of Phosphorus due to enhanced productivity are associated with peaks in accumulation of Phosphorus in sediments at the onset of the Oceanic Anoxic Event during the Cenomanian-Turonian boundary (OAE2) (Mort et al., 2007). 2) Previous modeling work has suggested that when Phosphorus is released from deep sea sediments, a eutrophication event occurs which leads to anoxia when deep sea oxygen levels fall below a threshold (Wallman, 2003).

Phosphorus peaks have been seen in other cores (refer to the figure below) where P burial is reduced in OAE sediments in most cores while other cores show a peak during the OAE itself (Follmi, 1995; 1999; Lenton, 2003; Mort et al., 2007).

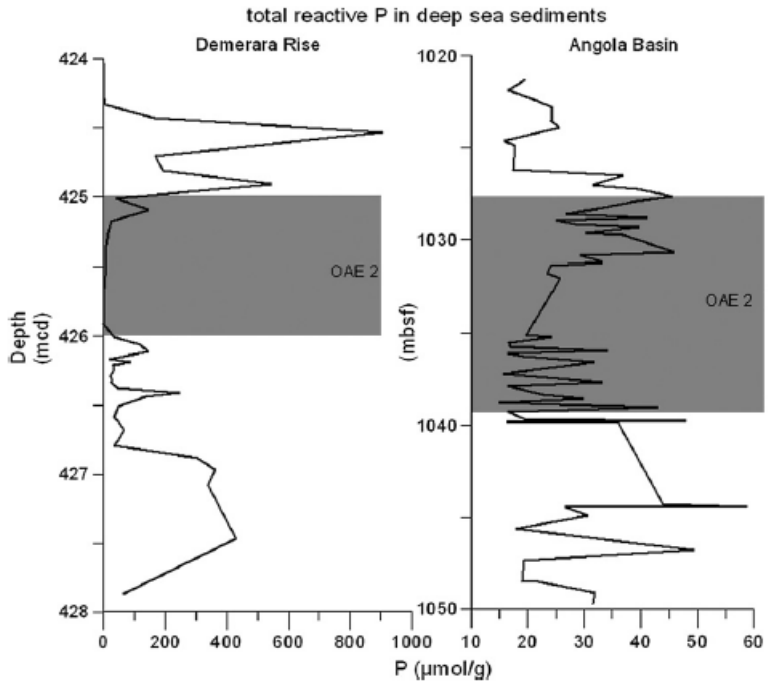


Figure 14 - Adapted from Kraal et al. (submitted for publication) and Tsandev and Slomp (2009): phosphorus concentrations vs. depth for other drilling sites DSDP 530 and ODP 1260.)

As discussed by Tsandev and Slomp (2009) the changes in oceanic Phosphorus is directly related to terrigenous erosion, and as the supply of reactive P increases so does primary productivity and carbon burial in the deep sea. Even though this influx is short lived, it has been determined that it is enough to trigger an oceanic anoxic event. Therefore, primary productivity is directly related to terrigenous erosion and runoff.

The relationship between Magnesium and Phosphorus supports the idea that the Phosphorus that is entering the ocean waters is originating from a terrigenous source since the influx of the heavy metal Magnesium typically originates from continents. The increased influx of these two elements into ocean waters can be attributed to surface erosion such as an increase in precipitation.

When comparing the general trends between Fe and S, it can be concluded that the increases in Sulfur concentrations are not associated with abundant pyrite formations since Fe and S do not share the same oscillations. Sulfur shares the same oscillations as Magnesium and Phosphorus, however. As discussed before, there was increased volcanic activity during the Cretaceous period. Massive amounts of outgassing in sub-aqueous volcanoes can provide increased Sulfur in deep ocean waters, but it does not explain the relation between S-Mg-P. Terrigenous volcanoes, however, could explain this relationship. Large amounts of outgassing caused by volcanic activity would emit vast amounts of particles in the atmosphere. These particles of ash, dust, and glass could then be used as a nucleus upon which atmospheric water can adhere to. Therefore, these volcanic particles can create clouds that would lead to precipitation. The increased precipitation would then lead to increased erosion of terrigenous rocks that would provide an influx of Phosphorus and Magnesium into ocean waters. The increase in Phosphorus could then trigger and terminate oceanic anoxic events in the Western Interior Seaway.

Magnesium and Sulfur compounds are also found in basaltic rocks in the form of $Mg^{2+}$ and $SO4^{2-}$. The major minerals that are found in basaltic rocks are olivine and pyroxene which are both chemically unstable in water and contain Magnesium. In high temperature hydrothermal systems, elemental compounds and minerals of Magnesium and Sulfur are removed from seawater and Calcium, Silica, and Potassium are added into the seawater. Therefore, the simultaneous precipitation of Magnesium and Sulfur can be explained by high temperature chemical reactions near a basaltic source rock.

Certain trace elements such as Zinc and Copper are redox sensitive and are enriched in anoxic sediments. Therefore, Zn and Cu can be used to define paleo environments. In an anoxic environment sediments are enriched in redox-sensitive trace elements because they are more soluble in oxidizing conditions and less soluble in reducing conditions. This is supported by the large peak of Zn at the Austin Chalk and Eagle Ford Shale contact when the depositional

environment became considerably more anoxic. Furthermore, these trace elements have been reported to be enriched in sediment by up to two to three orders of magnitude in black shales relative to those in grey shales (Algeo et al., 2003).

# Chapter 5

## Conclusions

Geochemical data accumulated with the use of ED-XRF was used to construct the chemostratigraphy of the Austin Chalk and Eagle Ford Shale. Furthermore, the geochemical data was then used as a proxy for various geologic and environmental processes.

1) Ca concentration was associated more with the Austin Chalk than the Eagle Ford, but the Eagle Ford still contained higher levels of Ca than standard black shales. Peaks in Si were indicative of the presence of quartz in both formations.

2) S-Mg-P relationship indicates minor anoxic events in the Western Interior Seaway which did not create vast amounts of black shales but did trigger abrupt changes in primary productivity and chemical variations in sediments.

3) Associations between Ti, Fe, and Al were used as proxies for sediment size and provenance of elements (detrial, terrigenous, or biological). The positive correlation indicated that the provenance of these elements came from both terrigenous erosion and biological activity.

4) The Eagle Ford Shale was deposited under anoxic to euxinic conditions as indicated by the increase in clay content and redox-sensitive trace elements.

References

Adams, D.D., Hurtgen, M.T., Sageman, B.B., 2010. Volcanic triggering of a biogeochemical cascade during Oceanic Anoxic Event 2. Nature Geoscience 3, 201e204.

Algeo, T.J., Maynard, J.B., 2004. Trace-metal behavior and redox facies in core shales of Upper Pennsylvanian Kansas-type cyclothems. Chemical Geology, 206; 289-318.

Algeo, T.J., Maynard, J.B., 2008. Trace-metal covariation as a guide to water-mass conditions in ancient anoxic marine environments. Geosphere. Oct 2008, v. 4, no. 5; 872-887.

Algeo, T.J., Rowe, H., Hower, J.C., Schwark,L., Hermann, A., Heckel, P., 2008. Changes in ocean denitrification during Late Carboniferous glacial-interglacial cycles. Nature Geoscience. v.1, October 2008; pp. 709-714.

Algeo, T.J., Rowe, H., 2011. Paleoceanographic applications of trace-metal concentration data. Chemical Geology, In Press, Available online 9 September 2011, ISSN 0009-2.

Algeo, T.J., Tribovillard, N. 2009. Environmental analysis of paleoceanographic systems based on molybdenum-uranium covariation. Chemical Geology. 268; 211-225.

Allard, B. "Trace Elements in Natural Waters." *Groundwater* (1995): 151-76.

Andrew, A.S, Whitford, D.J., and Hamilton, P.J., 1996. Application of chemostratigraphy to petroleum exploration and field appraisal: An example from the Surat Basin, Society of Petroleum Engineers, Document ID 37008-MS, SPE Asia Pacific Oil and Gas Conference, 28-31 October 1996, Adelaide, Australia, 978-1-55563-419-3.

Arthur, M.A.,Dean,W.E.,Schlanger,S.O.,1985.Variationsintheglobalcarbon cycle duringtheCretaceousrelatedtoclimate,volcanism,andchangesin atmospheric CO2. In:Sundquist,E.T.,Broecker,W.S.(Eds.),Thecarboncycle and atmosphericCO2: NaturalvariationsArcheantopresent.American Geophysical UnionGeophysicalMonograph,pp.504–529.

Barrera, E., Savin, S.M., 1999. Evolution of late Campanian–Maastrichtian marine climates and oceans. Geological Society of America Special Paper 332, 245–282.

Barron, E.J.,1983.Awarm,equableCretaceous—the natureoftheproblem.Earth- Sci. Rev.19,305–338.

Barron, E.J., 1985. Numerical climate modeling, a frontier in petroleum source rock prediction: results based on Cretaceous similuations. AAPG Bull.-Am. Assn. Petrol. Geol. 69, 448–459.

Berner, R.A., Lasaga, A.C., Garrels, R.M., 1983. The carbonate-silicate geochemical cycle and its effect on atmospheric carbon-dioxide over the past 100 million years. Am. J. Sci. 283, 641–683.

Brandes, Paul T. "Early Exploration on the Keweenaw Peninsula, Michigan." MinDat, 27 May 2008. Web. 30 Jan. 2013. Craig, James R., David J. Vaughtan, and Brian J. Skinner. “Resources of the Earth: Origin, Use, Environmental Impact, 3rd ed. Upper Saddle River, NJ: Prentice Hall, 2001.

Brumsack, H.J., 2006. The trace metal content of recent organic carbon-rich sediments: Implications for Cretaceous black shale formation, Elsevier, Paleogeography, Paleoclimatology, Paleoecology 232; 344-361.

Beckmann, B., Flögel, S., Hofmann, P., Schulz, M., Wagner, T., 2005a. Orbital forcing of Cretaceous river discharge in tropical Africa and ocean response.Nature 437, 241–244.

Brumsack, H.J., 2006. The trace metal content of recent organic carbon-rich sediments: Implications for Cretaceous black shale formation, Elsevier, Paleogeography, Paleoclimatology, Paleoecology 232; 344-361.

Cadrin, A.A.J., Kyser, T.K., Caldwell, W.G.E., Longstaffe, F.J., 1996. Isotopic and chemical compositions of bentonites as paleoenvironmental indicators of the Cretaceous Western Interior Seaway. Palaeogeogr. Palaeoclimatol. Palaeoecol. 119, 301–320.

Caldwell, W.G.E, Kauffman, E.G. (Eds.), Evolution of the Western Interior Basin, Spec. Pap.-Geol. Assoc. Can., vol. 39, pp. 333–353.

Caldwell, W.G.E, Kauffman, E.G. (Eds.), Evolution of the Western Interior Basin, Spec. Pap.-Geol. Assoc. Can., vol. 39, pp. 355– 378.

Cannon, W.F., and Force, E.R., 1986, Descriptive model of sedimentary Mn: U.S. Geological Survey Bulletin 1693, p. 231.

Caplan, M.L. and Bustin, R.M., 1998. Paleoceanographic controls on geochemical characteristics of organic-rich Exshaw mudrocks: role of enhanced primary productivity. Org. Geochem. 30; 161-188.

Chilvers, D. C., and P. J. Peterson. 1987. “Global Cycling of Arsenic.” In T. C. Hutchinson and K. M. Meema, eds., Lead, Mercury, Cadmium and Arsenic in the Environment. Scientific Committee on Problems of the Environment (SCOPE) 31. New York: John Wiley & Sons.

Clarke, L.J., Jenkyns, H.C., 1999. New oxygen isotope evidence for long-term Cretaceous climatic change in the Southern Hemisphere. Geology 27, 699–702.

Cruse, A.M., Lyons, T.W., 2004. Trace metal records of regional paleoenvironmental variability in Pennsylvanian (Upper Carboniferous) black shales. Chemical Geology 206, 319-345.

Davies-Vollum, K.S., 1997. Early Palaeocene palaeoclimatic inferences from fossil floras of the western interior, USA. Palaeogeogr. Palaeoclimatol. Palaeoecol. 136, 145–164.

Dawson, William C. "Limestone Microfacies and Sequence Stratigraphy: Eagle Ford Group (Cenomanian-Turonian) North-Central Texas Outcrops." *Gulf Coast Association of Geological Societies Transactions* 47 (1997): 99-105. *AAPG Datapages/Archives*. Web. 2 Feb. 2013.

Dawson, William C. "Shale Microfacies: Eagle Ford Group (Cenomanian-Turonian) North-Central Texas Outcrops and Subsurface Equivalents." *Gulf Coast Association of Geological Societies Transactions* 50 (2000): 607-21. *AAPG Datapages/Archives*. Web. 2 Feb. 2013.

Dawson, William C., and William R. Almon. "Eagle Ford Shale Variability: Sedimentologic Influences on Source and Reservoir Character in an Unconventional Resource Unit."*AAPG Datapages/Archives*. AAPG, 2010. Web. 2 Feb. 2013.

Dawson, William C., and Donald F. Reaser. "Trace Fossils in Middle and Upper Austin Chalk near Dallas, Texas--Paleoecological and Economic Significance." *The AAPG/Datapages Combined Publications Database* 69.1 (1985): 143. Abstract. (n.d.): n. pag. Print.

Dawson, W.C., and Reaser, D.F., 1990, Trace fossils and paleoenvironments of lower and middle Austin Chalk (Upper Cretaceous), north-central Texas: Transactions—Gulf Coast Association of Geological Societies, v. 40, p. 161–173.

De Gracianski, P.C., Deroo, G., Herbin, J.P., Montadert, L., Muller, C., Schaaf, A., Sigal, J., 1984. Ocean-wide stagnation episode in the late Cretaceous. Nature 308, 346-349.

Dean, W.E. and Arthur, M.A., 1989. Iron-Sulfur-Carbon relationships in organic-carbon-rich sequences I Cretaceous Western Interior seaway, American Journal or Science, Vol. 289; 708-743.

Demiason, G.J. Moore, D.T., 1980. Anoxic environments and oil source bed genesis. AAPG Bull. 64; 1179-1209.

Dravis, Jeff. "Depositional Setting and Porosity Evolution of the Upper Cretaceous Austin Chalk Formation South-Central Texas." *The AAPG/Datapages Combined Publications Database* 24.1 (1981): 3-5. *Archives Data Pages*. Web. 2 Feb. 2013.

Dravis, J.J., 1979, Sedimentology and diagenesis of Upper Cretaceous Austin Chalk Formation, south Texas and northern Mexico: Houston, Texas, Rice University, PhD dissertation, 513 p.

Douglas, R.G., Savin, S.M., 1975. Oxygen and carbon isotope analyses of Tertiary and Cretaceous macrofossils from the Shatsky Rise and other sites in the North Pacific Ocean. Initial Rep. Deep Sea Drilling Proj. 32, 509–520.

Eby, G. *Principles of Environmental Geochemistry*. Belmont: Brooks/Cole, 2004. Print.

Ellwood, Michael, and Constant Van Den Berg. "Zinc Speciation in the Northeaster Atlantic Ocean." Department of Earth Science, University of Liverpool, 23 July 1999.

Erba, E., 2004. Calcareous nannofossils and Mesozoic oceanic anoxic events. Mar. Micropalontol. 52, 85-106.

Erbacher, J., Huber, B.T., Norris, R.D., Markey, M., 2001. Increased thermohaline stratification as a possible cause for an ocean anoxic event in the Cretaceous period. Nature 409, 325-327.

Fitton, G., 1997. X-ray fluorescence spectrometery. In: Gill, Robin (Ed.),Modern Analytical Geochemistry. Addison Wesley Longman. 329 pp.

Fischer, A.G., Arthur, M.A., 1977. Secular variations in the pelagic realm. In: Cook, H.E. (Ed.), Deep-water carbonate environments. In: SEPM (Society for Sediment Geology), vol. 25. Special Publication, Tulsa, pp. 19-50.

Fischer, C.G., Arthur, M.A., 2002. Water mass characteristics in the Cenomanian US Wester Interior seaway as indicated by stable isotopes of calcareous organisms. Palaeogeogr. Palaeoclimatol. Palaeoecol. 188, 189– 213.

Follmi, K.B., 1995. 160 m.y. record of marine sedimentary phosphorus burial: coupling of climate and continental weathering under greenhouse and icehouse conditions. Geolgoy 23, 859-862.

Follmi, K.B., 1999. The phosphorus cycle, phosphogenesis and marine phosphate-rich deposits. Earth Sci. Rev. 40, 55-124.

Forester, R.W., Caldwell, W.G.E., Oro, F.H., 1977. Oxygen and carbon isotopic study of ammonites from the Late Cretaceous Bearpaw Formation in the southwestern Saskatchewan. Can. J. Earth Sci. 14, 2086– 2100.

Goldschmidt, V.M. "Geochemistry." *Geochemistry* (1958): 730. *Oxford University Press*.

Habicht, J.K.A., 1979. Paleoclimate, paleomagnetism, and continental drift. Am. Assoc. Petrol. Geol. Geol. Stud. 9, 110.

Hancock, J.M., Kauffman, E.G., 1979. The great transgressions of the Late Cretac- eous. J. Geol. Soc. London 136, 175–186.

Handoh, I.C., Lenton, T.M., 2003. Periodic mid-Cretaceous Oceanic Anoxic Events linked by oscillations of the phosphorus and oxygen cycles. Global Biogeochemical Cycles 17, 1092. doi:10.1029/2003GB002039.

Haug, G.H., Hughen, K.A., Sigman, D.M., Peterson, L.C., Röhl, U., 2001. Southward migration of the intertropical convergence zone through the holocene. Science 293,1304–1308.

Hovorka, S.D., and Nance, H.S., 1994, Dynamic depositional and early diagenetic processes in a deep-water shelf setting, Upper Cretaceous Austin Chalk, north Texas: Transactions—Gulf Coast Association of Geological Societies, v. 44, p. 269–276.

Hay, W.W., 2008. Evolving ideas about the Cretaceous climate and ocean circula- tion. Cretaceous Res. 29, 725–753.

He, S., Kyser, T.K., Caldwell, W.G.E., 1996. Stable isotope geochemistry of molluscan fossils of the Cretaceous marine cyclothem of the Western Interior Basin of North America: implications for paleoenvironments and paleoclimates. 30th IGC Abstract v3, Beijing, p. 78.

He, S.,Kyser,T.K.,Caldwell,W.G.E.,2005.PaleoenvironmentoftheWestern Interior Seawayinferredfrom d18O and d13C valuesofmolluscsfromthe Cretaceous Bearpawmarinecyclothem.Palaeogeogr.Palaeoclimatol.Palaeoe- col. 217,67–85.

Hentz, Tucker F., and Stephen C. Ruppel. "Regional Lithostratigraphy of the Eagle Ford Shale: Maverick Basin to East Texas Basin." *Gulf Coast Association of Geological Societies Transactions* 60 (2010): 325-37. Print.

Herman, A.B., Spicer, R.A., 1997. New quantitative palaeoclimate data for the Late Cretaceous Arctic: evidence for a warm polar ocean. Palaeogeogr. Palaeoclimatol. Palaeoecol. 128, 227–251.

Hofmann, P.,Wagner, T., Beckmann, B., 2003. A millennial- to centennial-scale record of African climate variability and organic carbon accumulation in the Coniacian–Santonian eastern tropical Atlantic (Ocean Drilling Program Site 959, off Ivory Coast and Ghana). Geology 31, 135–138.

Hovorka, S.D., and Nance, H.S., 1994, Dynamic depositional and early diagenetic processes in a deep-water shelf setting, Upper Cretaceous Austin Chalk, north Texas: Transactions—Gulf Coast Association of Geological Societies, v. 44, p. 269–276.

Hu, X.M., Wagreich,M., Yilmaz, I.O., 2012. Marine rapid environmental/climatic change in the Cretaceous greenhouse world. Cretac. Res. 38, 1–6.

Huber, B.T., Hodell, D.A., Hamilton, C.P., 1995. Middle–Late Cretaceous climate of the southern high latitudes: stable isotopic evidence for minimal equator-to- pole thermal gradients. Geol. Soc. Am. Bull. 107, 1164–1191. Huber, B.T., Norris, R.D., MacLeod, K.G., 2002. Deep-sea paleotemperature record of extreme warmth during the Cretaceous. Geology 30, 123–126.

Huber, B.T., Norris, R.D., MacLeod, K.G., 2002. Deep-sea paleotemperature record of extreme warmth during the Cretaceous. Geology 30, 123–126.

Huckriede, H. and Meischner, D. Origin and environment of manganese-rich sediments within black-shale basins, Geochimica et Cosmochimica Acta, Volume 60, Issue 8, April 1996, 1399-1413.

Jansen, J.H.F., Van der Gaast, S.J., Koster, B., Vars, A.J., 1999. CORTEX, a shipboard XRFscanner for element analyses in split sediment cores. Marine Geology 151, 143–153.

Jenkyns, H.C., 1980. Cretaceous anoxic events-from continents to oceans. J. Geol. Soc. Lond. 137, 171–188.

Jordan, T., 1981. Thrust loads and foreland basin evolution, Cretaceous, Western United States. American Association of Petroleum Geologists, Bulletin 65, 2506–2520.

Kauffman, E.G., 1977. Upper Cretaceous cyclothems, biotas and environments, Rock Canyon Anticline, Pueblo, Colorado. In: Kauffman, E.G. (Ed.), Cretaceous Facies, Faunas and Paleoenvironments across the Western Interior Basin: Mountain Geologist, 14, pp. 129–152. 34.

Kauffman, E.G., 1984. Paleobiogeography and evolutionary response dynamic in the Cretaceous Western Interior Seaway of North America. In: Westermann, G.E.G., (Ed.), Jurassic–Cretaceous Biochronology and Biogeography of North America. Geological Association of Canada, Special Paper 27, pp. 273–306.

Kraal, P., Slomp, C.P., Foster, A., Kuypers, M.M.M., submitted for publication. Phosphorus cycling from the margin to abyssal depths in the proto-Atlantic during oceanic anoxic event 2. Paleogeography Paleoclimatology Paleoecology.

Kujau, A., Nürnberg, D., Zielhofer, C., Bahr, A., Röhl, U., 2010. Mississippi River discharge over the last 560,000 years — indications from x-ray fluorescence core-scanning.

Kyser, T.K., Caldwell, W.G.E., Whittaker, S.G., Cadrin, A.J., 1993. Paleoenvironment and geochemistry of the northern portion of the Western Interior Seaway during Late Cretaceous time. In: Caldwell, W.G.E, Kauffman, E.G. (Eds.), Evolution of the Western Interior Basin, Spec. Pap.-Geol. Assoc. Can., vol. 39, pp. 355– 378.

Lahman, H.S., and J.B. Lassiter III. “The Evolution and Utilization of Marine Mineral”.

Larson, R.L., 1991. Latest pulse of Earth: evidence for a mid-Cretaceous superplume. Geology 19, 547-550.

Mancini, E.A., Parcell, W.C., Puckett, T.M., and Benson, D.J., 2003, Upper Jurassic (Oxfordian) Smackover carbonate petroleum system characterization and modeling, Mississippi interior salt basin area, northeastern Gulf of Mexico, USA: Carbonates and Evaporites, v. 18, no. 2, p. 125–150.

Mancini, E.A., Goddard, D.A., Barnaby, Roger, and Aharon, Paul, 2006a, Resource assessment of the in-place and potentially recoverable deep natural gas resource of the onshore interior salt basins, north central and northeastern Gulf of Mexico: U.S. Department of Energy Final Technical Report, Project Number DE-FC26-03NT41875, 173 p.

Markwick, P.J., 1998. Fossil crocodilians as indicators of Late Cretaceous and Cenozoic climates: implications for using palaeontological data in reconstruct- ing palaeoclimate. Palaeogeogr. Palaeoclimatol.Palaeoecol. 137, 205–271.

McDonough, K.J., Cross, T.A., 1991. Late Cretaceous sea level from a Paleoshoreline. J. Geophys. Res. 96, 6591–6607.

McNeil, D.H., Caldwell, W.G.E., 1981. Cretaceous rocks and their foraminifera in the Manitoba escarpment. Geological Association of Canada, Special Paper 21, 1–439.

Miall, A.D., Catuneanu, O., Vakarelov, B.K., Post, R., Andrew, D.M., 2008. The Western Interior Basin, Sedimentary Basins of the World. Elsevier, pp. 329– 362.

Montgomery, S., 1991. Horizontal drilling in the Austin Chalk Part 1. Geology, drilling history and field rules. Petroleum Frontiers, 7(3); 44.

Mort, H.P., Adatte, T., Föllmi, K.B., Keller, G., Steinmann, P., Materab, V., Berner, Z., Stüben, D., 2007. Phosphorus and the roles of productivity and nutrient recycling during oceanic anoxic event 2. Geology 35, 483e486.

Murphy, A.E., Sageman, B.B., Hollander, D.J., Lyons, T.L., Brett, C.E., 2000. Black shale deposition and faunal overturn in the Devonian Appalachian Basin: clastic starvation, seasonal water column mixing, and efficient biolimiting nutrient recycling Paleoceanography 15; 280-291.

N., Rao S., and P. Prasad. "Phosphate Pollution in the Groundwater of Lower Vamsadhara River Basin, India." *Environmental Geology* 31.1-2 (1997): 117-22. Print.

Norrish, K., Hutton, J.T., 1969. An accurate x-ray spectrographicmethod for the analysis of a wide range of geological samples. Geochimica et Cosmochimica Acta 33, 431–453.

Orians, K.J., Bruland, K.W., 1986. The biogeochemistry of aluminum in Pacific Ocean. Earth Planet. Sci. Lett. 78; 397-410.

Piper, D. Z. and Calvert. S.E., 2009. A marine biogeochemical perspective on black shale deposition, Elsevier, Earth Science Reviews 95; 63-96.

Potts, P.J., Webb, P.C., 1992. X-ray fluorescence spectrometry. Journal of Geochemical Exploration 44, 251–296.

Pratt, L.M., 1983. Isotopic studies of organic matter and carbonate in mid-Cretaceous strata near Pueblo, Colorado. In: Kauffman, E.G. (Ed.), Depositional Environments and Paleoclimates of the Greenhorn Tectonoeustatic Cycle, Rock Canyon Anticline, Pueblo, Colorado. Penrose Conference on Cretaceous Paleoclimates, Field Excursion Guidebook, pp. 77– 98.

Pratt, L.M., Arthur, M.A., Dean, W.E., Scholle, P.A., 1993. Paleooceanographic cycles and events during the Late Cretaceous in the Western Interior Seaway of North America. In: Caldwell, W.G.E, Kauffman, E.G. (Eds.), Evolution of the Western Interior Basin, Spec. Pap. Geol. Assoc. Can., vol. 39,pp. 333–353.

Price, R.A., 1973. Large-scale gravitational flow of supracrustal rocks, southern Canadian Rockies. In: Delong, K.A., Scholten, R. (Eds.), Gravity and Tectonics. J. Wiley Publishing, NY, pp. 491–502.

Reimann, C., and P. Caritat. "Chemical Elements in the Environment. Factsheets for Geochemist and Environmental Scientist." *Geological Magazine* 137 (2000): 596.

Richter, T.O., Van der Gaast, S., Koster, B., Vaars, A., Gieles, R., de Stigter,H.C., Haas,H.D., van Weering, T.C.E., 2006. The Avaatech XRF core scanner: technical description and applications to NE Atlantic sediments. Geological Society, London. Special Publication
267, 39–50.

Rimmer, S.M., 2004. Geochemical paleoredox indicators in Devonian–Mississippian black shales, Central Appalachian Basin (USA). Chemical Geology 206, 373–391.

Rimmer, S.M., Thompson, J.A., Goodnight, S.A., Robl, T.L., 2004. Multiple controls on the preservation of organic matter in Devonian–Mississippian marine black shales: geochemical and petrographic evidence. Palaeogeogr. Palaeclimat. Palaeoecol. 215, 125–154.

Robison, C.R., 1997. Hydrocarbon source rock variability within the Austin Chalk and Eagle Ford Shale (Upper Cretaceous), East Texas, U.S.A. International Coal Geology, 34; 287-305.

Rowe, H., Loucks, R.G., Ruppel, S.C., Rimmer, S.M., 2008. Mississippian Barnett Formation, Fort Worth Basin, Texas: Bulk geochemical inferences and Mo-TOC constraints on the severity of hydrographic restriction. Chemical Geology, 257; 16-25.

Rowe, H., Hughes, N., Robinson, K., 2012. The quantification and application of handheld energy-dispersive x-ray fluorescence (ED-XRF) in mudrock chemostratigraphy and geochemistry. Chemical Geology, In Press, Available online 8 January 2012.

Royer, D.L., 2006. CO2-forced climate thresholds during the Phanerozoic. Geochim Cosmochimica Acta 70, 5665e5675.

Royer, D.L.,Berner,R.A.,Beerling,D.J.,2001.Phanerozoic atmospheric CO2 change: evaluating geochemical and paleobiological approaches. Earth-Sci.Rev. 54, 349–392.

Ryan, W.B.F., Cita, M.B., 1977. Ignorance concerning episodes of ocean-wide stagnation. Mar. Geol. 23, 197-215.

Sarmiento, J.L., Herbert, T.D., Toggweiler, J.R., 1988. Causes of anoxia in the world ocean. Global Biogeochem. Cycles. 2, 115-128.

Schlanger, S.O., Jenkyns, H.C., 1976. Cretaceous oceanic events: causes and consequences. Geol. Mijnb. 55, 179-217.

Schlanger, S.O., Arthur, M.A., Jenkyns, H.C., Scholle, P.A., 1987. The Cenomanian-Turonian Oceanic Anoxic event, I. Stratigraphy and distribution of organic carbon-rich beds and the marine delta 13 carbon excursion. In: Brooks, J., Fleet, A.J. (Eds.), Marine petroleum source rocks. In: Geological Society of London, Special Publications, vol. 26. Blackwell Science Publishing, Oxford, pp. 371-399.

Schouten, S., Hopmans, E.C., Forster, A., van Breugel, Y., Kuypers, M.M.M., Sinninghe Damsté, J.S., 2003. Extremely high sea-surface temperatures at low latitudes during the middle Cretaceous as revealed by archaeal membrane lipids. Geology 31, 1069e1072.

Schröder-Adams, C.J., Cumbaa, S.L., Bloch, J., Leckie, D.A., Craig, J., Seif El-Dein, S.A., Simons, D.J.H.A.E., Kenig, F., 2001. Late Cretaceous (Cenomanian to Campanian)paleoenvironmental history of the eastern Canadian margin of the Western InteriorSeaway: bonebeds and anoxic events. Palaeogeography, Palaeoclimatology,Palaeoecology 170, 261–289.

Shimmield, G.B., 1992. Can sediment geochemistry record changes in coastal upwelling paleoproductivity? Evidence from northwest Africa and the Arabian Sea. In: Summerhayes, C.P., Prell, W.L., Emeis, K.C. (Eds.), Upwelling Systems: Evolution Since the Early Miocene, Geol. Soc. Spec. Publ., vol.64; 29-46.

Sloan, L.C., Barron, E.J., 1990. ‘‘Equable’’ climates during Earth history? Geology 18, 489–492.

Tertian, R., Claisse, F., 1994. Principles of quantitative x-ray fluorescence analysis. Wiley, Chichester. 385 pp.

Tjallingii, R., Röhl, U., Kölling, M., Bickert, T., 2007. Influence of the water content on xray fluorescence core-scanning measurements in soft marine sediments. Geochemistry,Geophysics, Geosystems 8 (2) 12 pp.

Tourtelot, H.A., 1962. Preliminary investigation on the geological and chemical composition of the Pierre Shale, Great Plains region. U. S. Geol. Survey Prof. Pap., 390.

Tourtelot, H.A., 1964. Minor-element composition and organic carbon content of marine and nonmarine shales of late Cretaceous age in Western Interior of the United States. Geochim. Cosmochim. Acta 28, 1597–1604.

Tourtelot, H.A., Rye, R.O., 1969. Distribution of oxygen and carbon isotopes in fossils of Late Cretaceous Age, Western Interior Region of North America. Bull. Geol. Soc. Am. 80, 1903– 1922.

Tribovillard, N., Algeo, T.J., Lyons, T., Riboulleau, A., 2006. Trace metals as paleoredox and paleoproductivity proxies: An update, Elsevier, Chemical Geology 232; 12-32.

Tsandev, I., Slomp, C.P., 2009. Modeling phosphorus cycling and carbon burial during Cretaceous Oceanic Anoxic Events. Earth and Planetary Science Letters 286, 71e79.

Vail, P.R., Mitchum, R.M., Jr., and Thompson, Sam III, 1977, Seismic stratigraphy and global changes of sea level, part 4: Global cycles of relative changes of sea level, *in* Payton, C.E., ed., Seismic stratigraphy—Applications to hydrocarbon exploration: Tulsa, Okla., American Association of Petroleum Geologists Memoir, v. 26, p. 83–97.

Villiers, Stephanie De, and Bruce K. Nelson. "Detection of Low-Temperature Hydrothermal Fluxes by Sewater Mg and Ca Anomalies." *Science* 285.5428 (1999): 721-23. Print.

Wagner, T., Sinninghe Damsté, J., Hofmann, P., Beckmann, B., 2004. Euxinia and primary production in Upper Cretaceous eastern Equatorial Atlantic surface waters fostered orbital-driven formation of marine black shales. Paleoceanography 19, PA4099. doi: 10.1029/2003PA000898.

Wagner, T., Wallman, K., Herrle, J.O., Hofmann, P., Stuesser, L., 2007. Consequences of moderate 25,000 yr lasting emission of light $CO_2$ into the mid-Cretaceous ocean. Earth Planet. Sci. Lett. 259, 200-211.

Wallmann, K., 2003. Feedbacks between oceanic redox states and marine productivity: a model perspective focused on benthic phosphorus cycling. Global Biogeochemical Cycles 17 (1084). doi:10.1029/2002GB001968, 18 pp.

Wescott, W.A., and Hood, W.C., 1994, Hydrocarbon generation and migration routes in the East Texas Basin: American Association of Petroleum Geologists Bulletin, v. 78, p. 287–307.

Wignall, P.B., Maynard, J.R., 1993. The sequence stratigraphy of transgressive black shales. Source Rocks in a Sequence Stratigraphic Framework, Katz, B.J., Pratt, L. (Eds.), AAPG Stud. Geol. 37; 35-47.

Wignall, P.B., and R. Newton, 2001. Black shales on the basin marine: a model based on examples from the Upper Jurassic of the Boulonnais, northern France, Sedimentary Geology 144; 335-356.

Whittaker, S.G., Kyser, T.K., 1993. Variations in neodymium and strontium isotopic composition and REE content of molluscan shells from the Cretaceous Western Interior seaway. Geochim. Cosmochim. Acta 57, 4003–4014.

Whittaker, S.G., Kyser, T.K., Caldwell, W.G.E., 1987. Lithic geochemistry of the Claggett marine Cyclothem in south-central Saskatchewan. Can. J. Earth Sci. 25, 1554–1563.

Wooten, J.W., and Dunaway, W.E., 1977, Lower Cretaceous carbonates of central south Texas: a shelf-margin study, *in* Bebout, D.G., and Loucks, R.G., eds., Cretaceous carbonates of Texas and Mexico, applications to subsurface exploration: University of Texas Bureau of Economic Geology Report of Investigations no. 89, p. 71–78.

Zheng, Y., Anderson, R.F., Green, A. V., and Kuwabara, J, 2000. Authigenic molybdenum formation in marine sediments: A Link to pore water sulfide in the Santa Barbara Basin, Geochimica et Cosmochimica Acta, Vol.64, No.24; 4165-4178.

## Biographical Information

Zain Abdi graduated with a BS in Geology-Biology from University of Texas at Arlington in 2012. Knowing the importance of higher education, he stayed on to obtain his Master's Degree in Petroleum Geology under the supervision of Dr. Harold Rowe.